Journal of Hazardous Materials 459 (2023) 132160

Contents lists available at ScienceDirect

Journal of Hazardous Materials

journal homepage: www.elsevier.com/locate/jhazmat

A generic approach to construct pseudo components for oil weathering models

Xiaolong Geng [a,b,*], Christopher H. Barker [c], Amy MacFadyen [c], Michel C. Boufadel [d], Dalina L. Thrift-Viveros [c], Robert K. Jones [c], Caitlin O'Connor [c], Kenneth Lee [e]

[a] Department of Earth Sciences, University of Hawai'i at Mānoa, Honolulu, HI 96822, USA
[b] Water Resources Research Center, University of Hawai'i at Mānoa, Honolulu, HI 96822, USA
[c] Office of Response and Restoration, Emergency Response Division, National Oceanic and Atmospheric Administration, Seattle, WA 98133, USA
[d] Department of Civil and Environmental Engineering, New Jersey Institute of Technology, University Heights, Newark, NJ 07102, USA
[e] Department of Fisheries and Oceans, Dartmouth, Nova Scotia B2YA2, Canada

HIGHLIGHTS

- A pseudo-component approach is developed for modeling oil evaporative weathering.
- 16 pseudo-components constructed to model oil evaporation are tested with 899 oils.
- Empirical formulas are derived to estimate pseudo-components' density and viscosity.

GRAPHICAL ABSTRACT

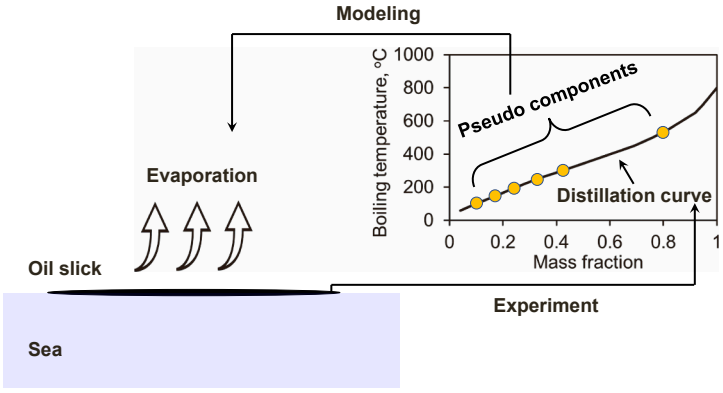

ARTICLE INFO

Editor: Baiyu Zhang

Keywords:
Oil evaporative weathering
Pseudo components
GNOME
ADIOS oil database
Numerical modeling

ABSTRACT

Oil weathering models are essential for predicting the behavior of spilled oil in the environment. Most models use a "Pseudo Component" (PC) approach to represent the wide range of compounds found in petroleum products. Within the approach, rather than modeling each individual compound in an oil, a manageable number of PCs are developed that represent whole classes of compounds. However, previous studies focused mainly on traditional crude oils and did not develop a generic approach to create an optimal set of PCs for a variety of oils. In developing the updates to the NOAA oil weathering model, we propose herein a generic approach to construct PCs using oil distillation data to capture the complexity of oil evaporative weathering. We validated our approach with 899 oils from the Automated Data Inquiry for Oil Spills (ADIOS) oil library and found that an optimal set of sixteen PCs should be used. These PCs include two with low boiling point (below 144 °C), one with a high boiling point (above 400 °C), and thirteen constructed within a middle range of boiling points with a

* Corresponding author at: Department of Earth Sciences, University of Hawai'i at Mānoa, Honolulu, HI 96822, USA.
E-mail address: gengxiaolong@gmail.com (X. Geng).

https://doi.org/10.1016/j.jhazmat.2023.132160
Received 21 April 2023; Received in revised form 15 July 2023; Accepted 25 July 2023
Available online 29 July 2023

temperature resolution of 20 °C. Our simulation tests suggested that this set of sixteen PCs adequately characterizes oil evaporation processes for a wide variety of oils.

1. Introduction

Oil Spills have been known to pose severe threats to marine biotic and abiotic environments worldwide [17,35,5]. In marine and coastal environments, spilled oil may enter the food chain of marine animals, sink to seafloor affecting marine vegetation, foul coastal infrastructures and damage nearshore habitats [18,2,28]. Response and contingency planning for oil spills relies on conducting numerical simulations to forecast probable trajectory and fate of oil in order to evaluate response options, oil toxicity and potential impacts on ecosystems [11,12,26,3,6]. Oil spilled in marine systems undergoes a complex array of physical, chemical, and biological processes [22,40]. These weathering processes include evaporation, photooxidation, dispersion, and emulsion, and they greatly alter oil properties, especially its density and viscosity [23, 24,38,42,43]. Evaporation is an important processes, and for light crude or refined oil products, evaporation could cause up to 75 % loss in volume in the first few days following marine oil spills [27]. Oil may also change chemically and physically when it evaporates on the sea surface [7]. Therefore, modeling oil evaporation processes has been recognized to be essential in an oil spill response in order to accurately forecast oil fate and transport after the spillage.

Oil is a complex mixture that usually contains thousands of organic compounds with different chemical and physical functionality. Therefore, characterizing oil evaporation processes is difficult as the composition of oil varies from source to source and even over time due to various weathering processes [9]. Major modeling efforts have been made over the past several decades to qualitatively and quantitatively investigate oil evaporation processes [4] was the first study that developed oil evaporation equations in which oil was assumed as a single component liquid and its overall vapor pressure was determined by oil distillation data. [27] simulated oil evaporation by using the classical water evaporation equations complemented with oil experiments. In their study, the mass transfer coefficient of oil was determined based on the experimental data of cumene evaporation. Subsequently, numerous studies were performed to explore the practical expressions for oil mass transfer coefficient (e.g., [8,37,19]). Payne and co-workers developed a so-called pseudo-component (PC) model to simulate oil evaporation [29, 31]. In their model, oil is represented as an ideal mixture of a relatively small number of components, named PCs. Each PC is characterized by a molecular mass, mole fraction, and a vapor pressure. The total evaporation rate of the mixture is set equal to the sum of the rate of the individual PCs. Similarly, [33] proposed a modeling procedure to estimate the extent of evaporative weathering experienced by crude oil. The essence of the procedure was to divide the crude oil into a series of pseudo-fractions by boiling point and model the evaporative behavior of each with an appropriate n-paraffin. Pseudo-component approach has been widely used in oil spill models, while the practical number of PCs determined by prior studies varied among different types of oils [20] constructed six PCs, representing BTEX, two PAH fractions, volatile aliphatics and two semi-volatile aliphatic fractions, respectively, to delineate oil evaporation process. The number of PCs has been greatly extended in recent studies for the sake of accurately representing the oils of interest (e.g., French McCay et al. [13]; [11]). For instance, in the OSCAR model, 25 PC groups were estimated using both the boiling point curve and GC data measured from the lab. Following the Deepwater Horizon oil spill, [39] coupled the Texas A&M Oilspill Calculator (TAMOC) to the oil application of the Connectivity Modeling Systems (oil-CMS) to capture both thermodynamic processes occurring in the near-field, meters above the wellhead, and the hydrodynamic processes in the far-field, up to kilometers away; 19 PCs were created in their simulations. In the SIMAP modeling of oil fate and mass balance for the Deepwater Horizon oil spill, 18 PCs were used including 9 soluble/semi-soluble and volatile/semi-volatile components defined by octanol-water partition coefficient, 8 insoluble and volatile/semi-volatile aliphatic components defined by boiling ranges and 1 residual oil component [11].

Regarding the construction of PCs, in much of the past literature and research, focus was on “traditional” crude oils, as these were the ones at most risk of major spills. Traditional crude oils generally have a linear distillation curve in the critical range of boiling points subject to evaporation in the environment. Optimizing the number of PCs to adequately model oil evaporative weathering processes has not been developed and thoroughly tested with a wide variety of oils. For instance, refined products and less “traditional” crudes, such as tight oils from the Bakken fields and blended products like Dilbit can have highly non-linear distillation curves. In developing the updates to the NOAA oil weathering model, in this paper we aim to revisit the selection of PC boiling points to find a minimal set that can still capture the complexity of oil evaporation. The layout of this paper is as follows: firstly, a generic approach to construct PCs based on oil distillation data is presented. The application scope of the proposed modeling approach is to simulate evaporative weathering of various types of oils with a uniform number of PCs selected. Secondly, using such approach, sets of PCs were constructed and tested with 899 oils from the Automated Data Inquiry for Oil Spills (ADIOS) Oil Database (https://adios.orr.noaa.gov/oils). Lastly, numerical simulations of oil evaporative weathering complemented with oil weathering data were conducted to explore the optimal set of PCs that can adequately capture oil evaporation as well as the practical formulas that can be used to estimate density and viscosity of individual PCs.

2. Methodology

2.1. General NOAA operational modeling environment (GNOME)

GNOME is a publicly available oil spill trajectory model that simulates oil movement and weathering due to winds, currents, tides and spreading [41]. GNOME has been under continuous development by NOAA’s Emergency Response Division for over twenty years. An oil weathering component, based on the previously developed Automated Data Inquiry for Oil Spills (ADIOS2) model has been incorporated since 2000 [21]. GNOME tracks the movement and weathering of an oil spill on water by dividing the spill volume into Lagrangian elements (i.e., LEs), which are each transported and weathered independently. Processes which result in movement of LEs are termed ‘movers’ in GNOME which are associated with currents, winds and diffusion. The movers are numerically expressed as sets of velocity components, which can be a field of vectors or a point vector, depending on data availability. The calculation of total movement is a simple vector addition of the displacement of a given LE by each mover over a time step. The overall amount of oil that is found on the water’s surface as a slick and that is found in the water column as droplets is calculated at the beginning of a model run by taking into account user-provided weather and sea state information. The initial mass and form of the oil (surface slick or subsurface droplets) is determined by input parameters based on the nature of the release. The oil weathering processes are considered based on manipulating specific weathering modules in GNOME (e.g., spreading, evaporation, biodegradation, dissolution, and emulsification) for each element individually based on the conditions at the time and location of that element.

2.2. Pseudo-component approach

Petroleum is a complex mixture of thousands of individual compounds. Therefore, it is impossible to characterize an oil down to the compound level, and it would be computationally impossible to model each compound individually. In the GNOME model, similarly to most known oil weathering models, a 'pseudo-component' (PC) approach is adopted, where crude oils and refined products are modeled as mixture of discrete non-interacting components. In the GNOME model, oil is divided into a small number of PCs that each represents a collection of similar compounds. For example, five PCs are constructed according to oil distillation data, each of which represents 20% of oil by mass. It allows to track how oil changes chemically and physically as its individual PCs interact with the environment in different ways.

In order to be a flexible framework, the weathering algorithms in GNOME can work with any number of PCs, each with a distinct set of properties [41]. Thus, a select number of PCs along with their properties can be determined to best represent an oil mixture for a specific application. An oil assay does not directly have the data for the PCs. Therefore, the effectiveness of the PC selection depends on the availability of oil data measurements. As oil is a mixture of many compounds with a wide range of boiling points, different fractions will boil off at different temperatures. This distillation process is used to refine petroleum into useful products, and thus distillation curve is commonly produced as part of oil analysis, which is used herein to construct PCs.

Also, the range of boiling points (BPs) have been considered in different ways due to different modeling needs. The low-BP fraction usually evaporates very quickly and thus can be considered as a single PC. The high-BP fraction is non-volatile and those compounds can be treated as a single PC as well. The fraction within the middle-range BP is moderately volatile, and thus an optimal resolution is essential. This is because a low resolution may not be able to precisely resolve oil evaporative weathering process, while an extremely high resolution, resulting in a huge number of PCs, would dramatically lower the computational efficiency of oil weathering models. The innovation of this paper is to develop a generic approach to construct PCs used for oil weathering modeling. The construction of PCs is determined by the boiling points of oil compounds, and classified into three categories: oil components with low BPs, middle-range BPs and high BPs, respectively. Two PCs were constructed at low BPs. The first one includes the fraction from the initial BP to 80 °C to represent the compounds with BPs lower than benzene. The second one includes the fraction from 80 °C to 144 °C to represent BTEX and whatever saturates fall in that range. One PC was constructed at a high BP to include the fraction of high BP compounds, and its representative BP is the average of the cutoff for high boiling temperature (e.g., 400 °C) and the terminal boiling temperature at which all the oil compounds boil off. To construct PCs within middle-range BPs, the middle range is first divided into multiple consecutive temperature cuts based on a temperature resolution (e.g., 20 °C). A PC is then constructed within each temperature cut, and its representative BPs are selected at the midpoints of the cut. The mass fractions of PCs are obtained by linear interpolation of oil distillation data with their representative BPs. Note that the PC approach presented herein is developed based on oil distillation curve. Therefore, a sufficient number of oil distillation measurements is essential to implement this approach for a specific type of oil. The schematics of how to construct PCs from oil distillation measurements along with an example of PCs constructed for the Alaskan North Slope (ANS) oil are shown in Fig. 1.

The molecular weight of PCs is calculated based on Equation (2.42) proposed in [36]:

$$MW = \left(\frac{1}{b}\left[a - \ln\left(T_\infty - T\right)\right]\right)^q \tag{1}$$

where MW and T represent the molecular weight in g/mol and temperature in K, respectively; the coefficients T_∞ a, b, and q depend on the

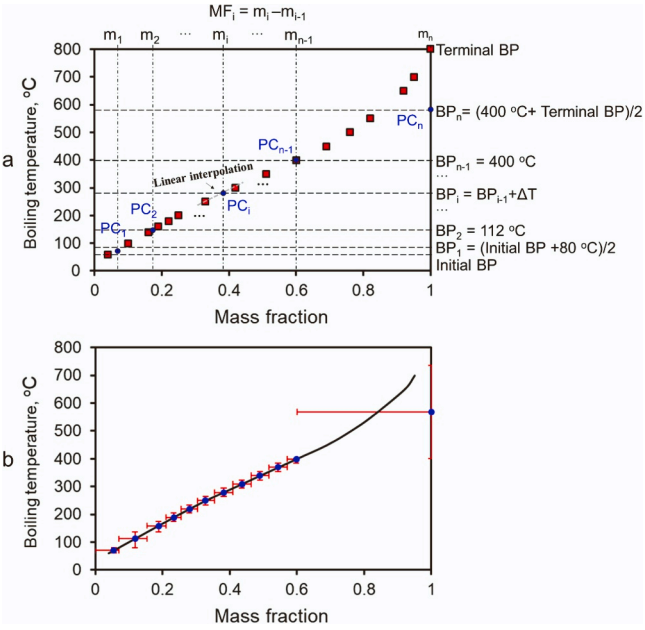

Fig. 1. : (a) schematic of the algorithm to construct pseudo components (PCs) based on oil distillation measurements. (b) Example construction of PCs for the Alaska North Slope (ANS) oil, where the temperature resolution and temperature cutoff for high boiling point (BP) are set at 30 °C and 400 °C, respectively. Red symbols shown in Fig. 1a represent the distillation measurement points. Red horizontal and vertical bars shown in Fig. 1b denote the representative range of mass fraction and boiling temperature for the PCs.

chemical structure of the component, which have been estimated in [36] for paraffinic, naphthenic, and aromatic hydrocarbon groups. Our simulation tests indicate that the calculation of molecular weight with different sets of coefficients produced nearly identical oil evaporation extent. Therefore, the average of the three hydrocarbon groups is simply used to compute the molecular weight of each PC.

The density and viscosity of PCs are estimated by third-order polynomial functions fitted to 58 ExxonMobil crude oil assays from the ADIOS Oil Database (Fig. 2). The oil records are reported in Table S1, labeled as EX00001 – EX00058. For each oil assay, key properties such as mass fraction, density viscosity, and distillation curve, were measured for fresh oil as well as its weathered fractions that boil off within 7 consecutive boiling cuts of [the initial BP, 15.56 °C], [15.56 °C, 73.89 °C], [73.89 °C, 165.56 °C], [165.56 °C, 248.89 °C], [248.89 °C, 343.33 °C], [343.33 °C, 537.78 °C] and [537.78 °C, the terminal BP], respectively. The oil was separated by fractional distillation, characterized as 'Butane and Lighter', 'Light Naphtha', 'Heavy Naphtha', 'Kerosene', 'Diesel 480', 'Vacuum Gas Oil', and 'Vacuum Residue'. Note that the terminal BP represents the temperature threshold at which all the oil compounds boil off, which varies among the oil assays (Table S1). The fitted polynomial functions can be used to estimate density and viscosity of individual PCs with their representative BPs. The overall oil density and viscosity are estimated by the mass- and molar-weighted averages of PCs, respectively, expressed as follows:

$$\rho = \sum_{i=1}^{N} m_i \rho_i \tag{2}$$

$$\ln(\nu) = \sum_{i=1}^{N} mol_i \ln(\nu_i) \tag{3}$$

Where ρ represents density of oil, and ρ_i and m_i represent density and mass fraction of the i_{th} PC, respectively; ν represents the kinematic viscosity of oil, and ν_i and mol_i represent kinematic viscosity and molar fraction of the i_{th} PC. Note that the molar fraction can be obtained by

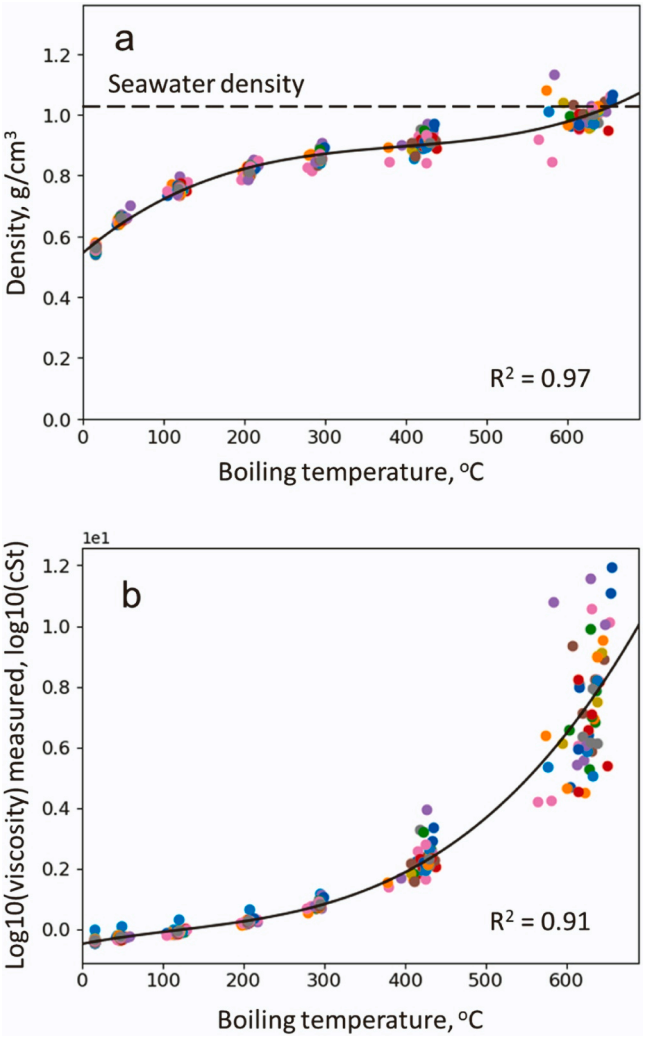

Fig. 2. : (a) Density and (b) logarithmic viscosity of oil weathered fractions measured within certain boiling cuts, along with their fitting curves using a 3rd-order polynomial function. Colored dots represent the measurements of 58 ExxonMobil oil assays recorded in the ADIOS Oil Database where density and viscosity are measured for fresh oil and its weathered fractions within the seven consecutive boiling cuts. Note that the integrated average within each boiling cut is used to denote its representative boiling temperature.

using the given mass fraction and molecular weight estimated with Eq. 1.

Eqs. 2 and 3 are further tested with the ExxonMobil oil assays, described as follows. For each oil assay, seven PCs are first constructed within the seven consecutive temperature ranges, representing oil weathered fractions within those boiling cuts. Then, the density and viscosity along with mass and molar fractions measured for each weathered oil fraction (i.e., each PC) were used as inputs for Eqs. 2 and 3 to estimate the density and viscosity of the fresh oil. The comparison between estimated and measured oil density and viscosity resulted in R^2 values of 0.98 and 0.87, respectively, indicating mass- and molar-weighted averages of PCs closely reproduce their corresponding oil density and viscosity measurements (Fig. 3).

A correction factor, $\frac{\rho_{measured,0}}{\sum_{i=1}^{N} m_{i,0}(a_1 T_i^3+b_1 T_i^2+c_1 T_i+d_1)}$, is introduced herein so that the initial estimation and measurement of the oil density are consistent when the PC approach is implemented in oil weathering modeling. The calibrated density for each PC will be used to compute the oil density based on updated mass fraction at each time step using Eq. 2. As a result, the empirical formula to estimate PC's density is expressed as

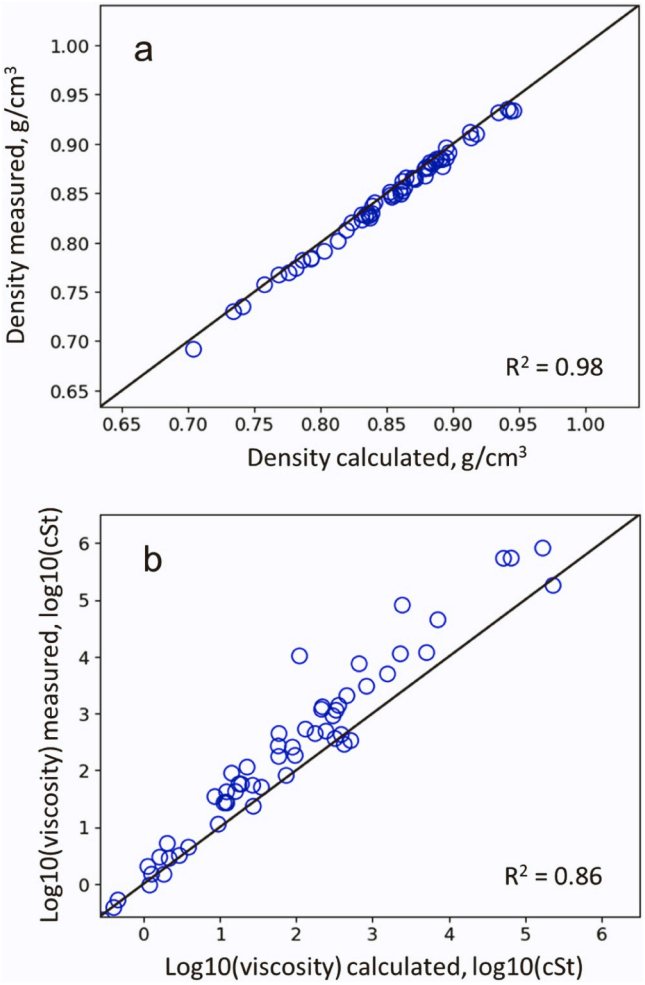

Fig. 3. : Comparison of measured and estimated density and viscosity of 58 ExxonMobil oils in the ADIOS Database.

follows:

$$\rho_i = \left(\frac{\rho_{measured,0}}{\sum_{i=1}^{N} m_{i,0}\left(a_1 T_i^3 + b_1 T_i^2 + c_1 T_i + d_1\right)}\right)\left(a_1 T_i^3 + b_1 T_i^2 + c_1 T_i + d_1\right) \quad (4)$$

Where $\rho_{measured,0}$ represents the initial oil density measurement, and $m_{i,0}$ and T_i represent the initial mass fraction and the representative BP of the i_{th} PC, respectively. The coefficients of the fitted polynomial function, (a_1, b_1, c_1, d_1), are estimated to be (4.38×10^{-9}, -5.17×10^{-6}, 2.25×10^{-3}, -5.44×10^{-1}).

Similarly, the empirical formula to estimate PC's viscosity is expressed as follows:

$$\ln(\nu_i) = \left(\frac{\ln\left(\nu_{measured,0}\right)}{\sum_{i=1}^{N} mol_{i,0}\left(a_2 T_i^3 + b_2 T_i^2 + c_2 T_i + d_2\right)}\right)\left(a_2 T_i^3 + b_2 T_i^2 + c_2 T_i + d_2\right) \quad (5)$$

Where $\ln(\nu_{measured,0})$ represents the logarithm of the initial oil viscosity measurement, and a correction factor, expressed as $(\frac{\ln(\nu_{measured,0})}{\sum_{i=1}^{N} mol_{i,0}(a_2 T_i^3+b_2 T_i^2+c_2 T_i+d_2)})$, is introduced for a match between initially measured and estimated oil viscosity. The coefficients of the fitted polynomial function, (a_2, b_2, c_2, d_2), are estimated to be (4.37×10^{-8},

-1.53×10^{-5}, 5.02×10^{-3}, -4.61×10^{-1}). The formulas along with the fitted coefficients for estimating oil density and viscosity are further validated with 152 oil assays from the ADIOS Oil Database, including 47 fresh oils and 105 their weathered ones (Table S2). For the validation, the density and viscosity of the weathered oils are first estimated with Eqs. 4 and 5, where PCs along with their density and viscosity are derived from the fresh oil measurements, and the mass and molar fractions of the PCs are obtained from the distillation measurements of the weathered oil assays. The estimated density and viscosity are then compared against their measurements (Fig. 4).

2.3. Oil evaporation algorithm in GNOME

In the GNOME model, each PC is treated as a single substance with an associated vapor pressure. The evaporation of each component is tracked separately, and the overall evaporation extent of oil mixture is the sum of the extent of individual PCs. Evaporation of volatile components is found from the solution of coupled simple differential equations. This is the same formulation as that adopted in ADIOS2 [21]:

$$\frac{dm_i}{dt} = -\left(1 - f_w\right)\frac{A \cdot K_i \cdot MW_i \cdot P_i}{RT_w}\frac{\frac{m_i}{MW_i}}{\sum \frac{m_i}{MW_i}} \tag{6}$$

where m_i is the mass of PC_i in the LE (in kg), f_w is the fractional water content in the emulsion, The parameter A represents the surface area associated that element (in m^2). It increases as oil spreads and reaches the maximum when the terminal oil thickness is obtained. Further details of the spreading algorithm within GNOME can be found in [41];.

P_i is the vapor pressure at the water temperature of PC_i (in Pa), R is the universal gas constant in SI units (8.3144 J/(K mol)), T_w is the water temperature (in K), and K_i is the mass transfer coefficient (in m/s) [27], expressed as.

$$K_i = c \cdot U_{10}^{0.78} \cdot S_c^{-2/3} \tag{7}$$

where $c = 0.0048$ is a constant, U_{10} is the wind speed at 10 m above water surface (in m/s), and S_c is Schmidt number, expressed as:

$$S_c = 1.38 \cdot \left(\frac{MW_{water}}{MW_i}\right)^{1/3} \tag{8}$$

The vapor pressure of the components, P_i, is derived from their boiling points using Antoine's equation [20,25]:

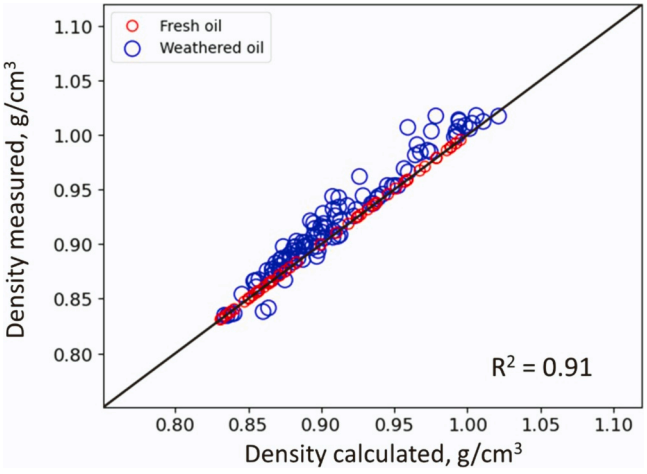

Fig. 4. : Comparison of measured and estimated density for 105 weathered oils. The estimation is based on Eq. 4 where the correction factor is obtained from the corresponding 47 fresh oils.

$$\ln \frac{P_i}{P_0} = \frac{\Delta S_i (BP_i - C)^2}{R \cdot BP_i}\left[\frac{1}{BP_i - C} - \frac{1}{T_w - C}\right] \tag{9}$$

Where P_0 represents atmospheric pressure, R is the gas constant, and the parameters $C = 0.19 \cdot BP_i$-18 and $\Delta S_i = 8.75 + 1.987 \log(BP_i)$.

The differential equations can be simplified as first-order decay equations:

$$\frac{dm_i}{dt} = -edc \cdot m_i \tag{10}$$

where edc represent the first-order decay rate, expressed as:

$$edc = \frac{(1 - f_w) A \cdot K_i \cdot P_i}{RT_w \sum \frac{m_i}{MW_i}} \tag{11}$$

The equation indicates the impacts of different environmental conditions on oil evaporative weathering process. Stronger winds likely accelerate oil evaporation process; an increase in water temperature rises the vapor pressure of oil components, which facilitates oil evaporation on the sea surface.

2.4. Numerical implementation

In order to explore the optimal number of PCs to characterize oil evaporative weathering process, sets of PCs were created with the temperature resolutions of 1 °C, 5 °C, 10 °C, 20 °C, 30 °C, and 50 °C, and the high-BP cutoffs of 400 °C, 500 °C, and 600 °C. The resulting number of PCs is reported in Table 1. For each set of PCs, oil evaporative weathering was simulated with the GNOME model. The simulations were conducted for 899 oils recorded in the ADIOS oil library (Table S3). Note that all the oils tested herein are publicly available through the web interface of the ADIOS Oil Database (https://adios.orr.noaa.gov/oils/). The simulations of oil evaporation included two scenarios with and without oil spreading: with spreading, oil spreading was incorporated by activating the spreading module in the GNOME model; without spreading, only oil evaporation was simulated by assuming that the oil surface area reaches its maximum immediately after the spillage.

3. Results and discussion

3.1. Density and viscosity estimation

Fig. 4 compares the oil density measured from the 152 oil assays to their estimates with Eq. 4. Note that for the estimation, PCs along with their density were estimated from fresh oil measurements, while the mass fractions of the PCs were obtained from corresponding oil distillation measurements. The value of R^2 is 0.91 for weathered oils, indicating the empirical formula proposed herein well captured the oil density change at varying degrees of evaporative weathering. The estimation of oil viscosity demonstrates the same robustness ($R^2 = 0.91$) for capturing the viscosity when oil becomes weathered (Fig. 5). However, relatively poor estimates are consistently observed for high viscosity oil subjected to relatively high degree of evaporative weathering,

Table 1
Number of PCs constructed with different temperature resolutions and thresholds for high BPs.

Temperature Resolution	High BP = 400 °C	High BP = 500 °C	High BP = 600 °C
50 °C	8	10	12
30 °C	12	15	18
20 °C	16	21	26
10 °C	29	39	49
5 °C	54	74	94
1 °C	259	359	459

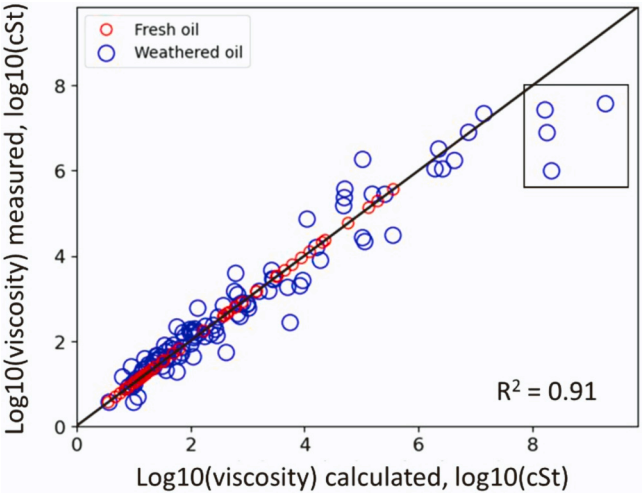

Fig. 5. : Comparison of measured and estimated viscosity for 105 weathered oils. The estimation is based on Eq. 5 where the correction factor is obtained from the corresponding 47 fresh oils. Note that relatively poor fitting is observed for high viscosity oil samples that are marked within a black box in the figure.

particularly for oil samples of Access West Blend Winter (product type: bitumen blend) with 25.3 % and 26.5 % evaporated and Heritage HE (product type: heavy crude) with 14.5 % and 16.3 % evaporated, bounded within a black box. This is most likely due to a relatively poor fitting of 3rd order polynomial function to the extremely high viscosity measured for the residual oil fraction with BPs above 537.78 °C; the viscosity measurements at high BPs, as shown in Fig. 2b, demonstrate a large variation among different oils, which negatively affects the goodness of fit to the high viscosity oils.

3.2. Evaporation of a two-component hydrocarbon mixture

Evaporation of a two-component hydrocarbon mixture was simulated herein to evaluate the functionality of the PC construction as well as the evaporation algorithm when different lengths of time step were adopted in the simulation. The hydrocarbon mixture was assumed to consist of two components with equal mass fraction (i.e., 50 %/50 %) but different BPs of 200 °C and 400 °C, respectively, each of which can be simply represented by a PC with corresponding BP and mass fraction. The temperature and wind speed used in the simulation were 20 °C and 1.0 m/s, respectively. Fig. 6a shows the evaporation extent of the individual PCs with time, neglecting oil spreading. The results demonstrate that the component with a low BP quickly evaporated within an hour, while the mass of the component with a high BP persisted over time. Apparently, a large time step (e.g., 1 h) did not capture the initial mass change of the low-BP component due to its extremely fast evaporation rate within the first hour. However, all the simulations to some extent converged at later time, indicating that relatively large time steps adopted in this paper (e.g., 1 h) are still feasible in the GNOME model to predict hydrocarbon evaporation at the time scale of interest. It is expected that the evaporation of the hydrocarbon mixture shows a two-phase change (Fig. 6b). A sharp decrease in its mass fraction occurred within the first hour due to the evaporation of the low-BP PC, followed by a persistent mass fraction of 50% over time due to extremely low evaporation rate of the high-BP PC. The results demonstrate nearly the same trend when oil spreading was simultaneously incorporated in the simulations (Fig. 6c and d). The oil evaporated slightly faster for the non-spreading case, which is most likely because the maximum area extent was adopted at the beginning of the simulations. Only a slight difference in mass fraction is observed when relatively large time steps were adopted in the simulation for both cases, indicating that with the presented evaporation algorithm, a reasonably large time step (e.g., 1 h) is allowed for predicting hydrocarbon evaporation processes.

3.3. Optimal number of pseudo components

Simulations were conducted to explore the optimal number of PCs that could adequately delineate oil evaporation processes. Taking the Heidrun crude oil as an example, sets of PCs were first constructed with different temperature resolutions and different cutoffs for high BPs (Fig. 7a and Fig. S1). Then, different sets of PCs were used as representatives of the oil to simulate its temporal evaporation extent. It shows that the number of PCs increased from 16 to 29 when the temperature resolution for the middle-BP components was elevated from 20 °C to 10 °C. Similarly, the number of PCs increased when a higher cutoff for high BPs was adopted. The number of PCs increased from 16 to 26 when the high-BP cutoff was elevated from 400 °C to 600 °C (Fig. S2). This is expected because the range of temperature becomes wider when a higher cutoff is adopted, which subsequently results in more PCs created. The simulated evaporation extent shows that evaporation started from the PCs with lower BPs, which is observed by earlier falling of the mass fraction curves (Fig. 7b). With a higher number of PCs, the change of the mass fraction was delineated at a finer time scale. Fig. 7c-d shows the evaporation extent for the Heidrun crude oil simulated by the PCs constructed with different temperature resolutions. The temperature resolution of 50 °C, 30 °C, 20 °C, 10 °C, 5 °C, and 1 °C resulted in 8, 12, 16, 29, 55, and 258 PCs, respectively. The simulated evaporation extent for the cases with the temperature resolutions of 50 °C and 30 °C seemed to underestimate the oil evaporation rate. The simulations for the cases with the temperature resolutions of 20 °C, 10 °C, 5 °C and 1 °C predicted nearly the same evaporation extent, indicating 20 °C could be used as the optimal resolution to construct the PCs for modeling oil evaporation. Figs. 7e-7f show the simulated evaporation extents of the Heidrun crude oil when different cutoffs for high BPs were used to construct PCs. Nearly the same evaporation extent proves that a cutoff of 400 °C for high BPs is adequate for constructing PCs to model oil evaporative weathering.

3.4. Application of the PC approach to oils in the ADIOS database

The PC approach along with the oil evaporation algorithm were further tested with all available 899 oil records from the ADIOS Oil Database. The oils are categorized into 14 groups in the database, including crude oil, tight oil, condensate, bitumen blend, bitumen, refined product, fuel oil, distillate fuel oil, residual fuel oil, refinery intermediate, solvent, bio-petro fuel oil, lube oil and dielectric oil. For each oil record, sets of PCs were constructed with different temperature resolutions (i.e., 1 °C, 5 °C, 10 °C, 20 °C, 30 °C, and 50 °C) and different cutoffs for high BPs (i.e., 400 °C, 500 °C, and 600 °C). Fig. 8a lists examples of PCs constructed within each oil category. The figure shows that the oil distillation curve within the critical range of BPs could be significantly nonlinear and high variable among different oil categories. The simulated evaporation extent indicates a strong correlation between the desired temperature resolution of PCs for accurately capturing oil evaporation process and the range of oil boiling temperature (Fig. 8b). The oil with a wider boiling temperature range exhibited very close predictions of evaporation extent by the PCs constructed with the temperature resolution varying from 1 °C to 30 °C (e.g., NO00046, AD02070, and EX00540). In contrast, the simulated evaporation extent by different temperature resolution demonstrates a remarkable difference for the oil with a relatively narrow boiling temperature range (e.g., AD01654, EC03629, and AD02098). This is expected as a narrower boiling temperature range implies more oil mass loss per unit increase in temperature; therefore, in order to capture the same loss in oil mass, a finer temperature resolution needs to be required.

Fig. 9 shows % discrepancy of simulated evaporation extent when the temperature resolution used to construct PCs decreases from 1 °C to

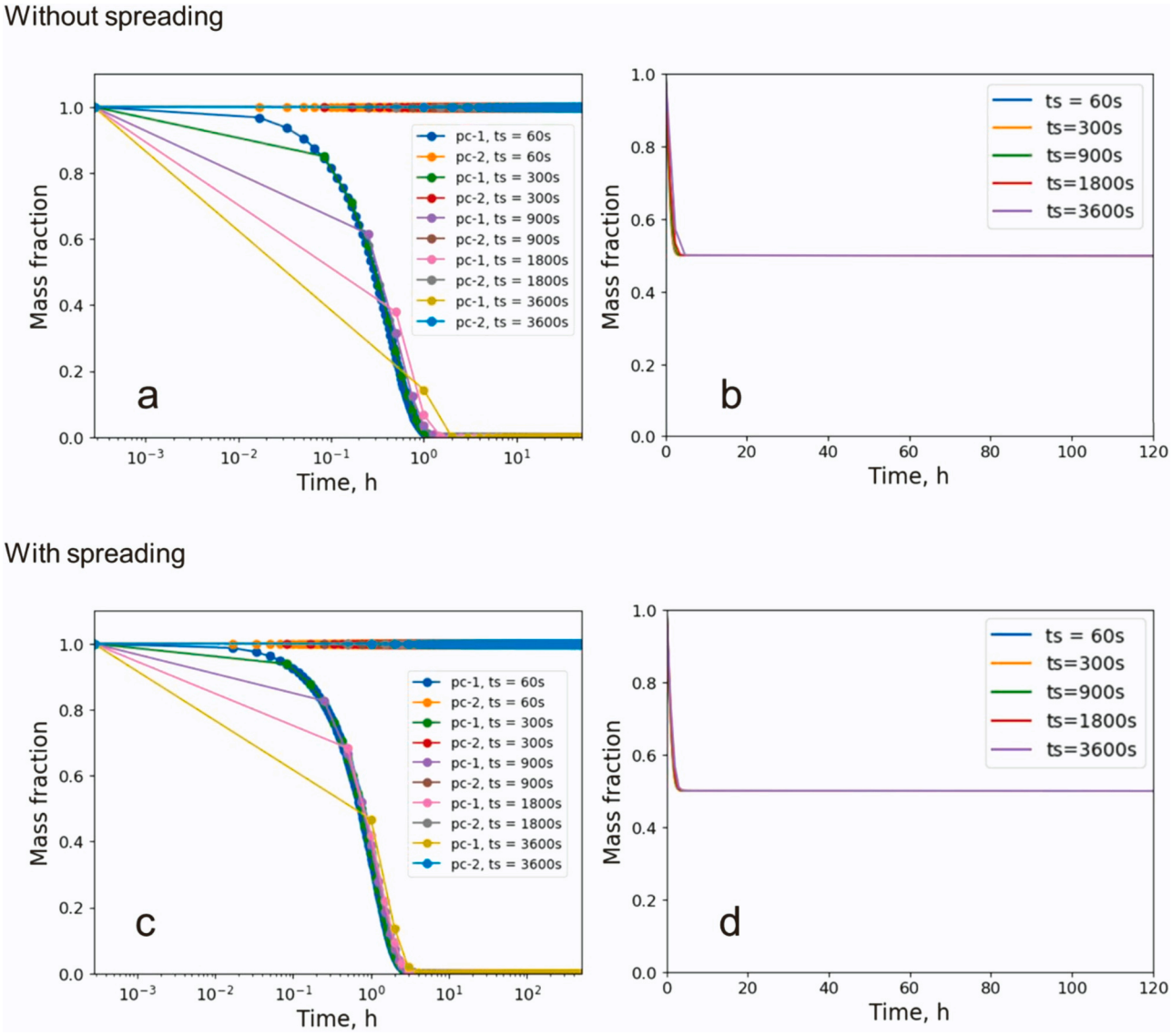

Fig. 6. : Simulated evaporation extent of the PCs and hydrocarbon mixture as a function of time using different length of time step (a-b) without and (c-d) with oil spreading, respectively. Note that the hydrocarbon mixture is assumed to consist of two components with equal mass fraction but different boiling points of 200 °C and 400 °C, respectively.

a coarse resolution. It is expected that the finer the temperature solution became, the less the discrepancy was. When the temperature resolution changed from 1 °C to 20 °C with/without oil spreading, the discrepancy of the simulated evaporation extent was consistently less than 10 % for all the oil categories, but the number of PCs dramatically dropped nearly 16 times from 258 to 16. The reduced number of PCs implies significant improvement in the modeling efficiency as each PC is presented as an ordinary differential equation in the GNOME model that needs to be iteratively solved at each time step for modeling oil evaporative weathering. Our results indicate that a selection of 20 °C as the temperature resolution for constructing PCs would be reasonable to forecast oil evaporation extent, at least from oil response perspective where transport and weathering extent of oil needs to be forecast instantly after oil spillage. Similarly, our simulations for high-BP cutoffs shows that elevating the threshold from 400 °C to a higher temperature threshold (e.g., 500 °C and 600 °C) only caused about 1% discrepancy in mass (Fig. 10). It concludes that a cutoff of 400 °C for high BPs is adequate for constructing PCs to delineate oil evaporative weathering for all the oil categories tested in this paper. This is most likely because the oil compounds with BPs above 400 °C hardly evaporate, as shown in Fig. 6. These findings are further proved by statistical analysis of the oil categories with over 10 oil records (Fig. 11). Box plots show that the mean and median of the % discrepancy for these oil categories were controlled within 2 % when 20-°C temperature resolution is adopted for PC construction with/without oil spreading. The corresponding 75th and 95th percentiles were controlled within 4% and 7%, respectively. Pseudo-component approach has been introduced in oil weathering modeling since 1983 proposed by Payne and co-workers [30–32]. Distillation measurements are very common for oil characterization due to their crucial role in operating refineries. Thus, for oil spill modeling, pseudo components are usually constructed by dividing oil into a series of pseudo-fractions by BPs [e.g., [20,33]; French McCay et al., [13]; [11]]. While the PC approach has been studied over the past two decades, the optimal number of PCs designated for oil spill modeling varied significantly among studies due to different environmental scenarios and oil types they dealt with. The PC approach proposed in this study is generic as the number of PCs is determined by a user-defined temperature resolution and cutoff for high BPs. In addition, our simulation tests with 899 oils from the ADIOS database suggest an optimal number of 16 PCs to adequately capture oil evaporative weathering from oil response

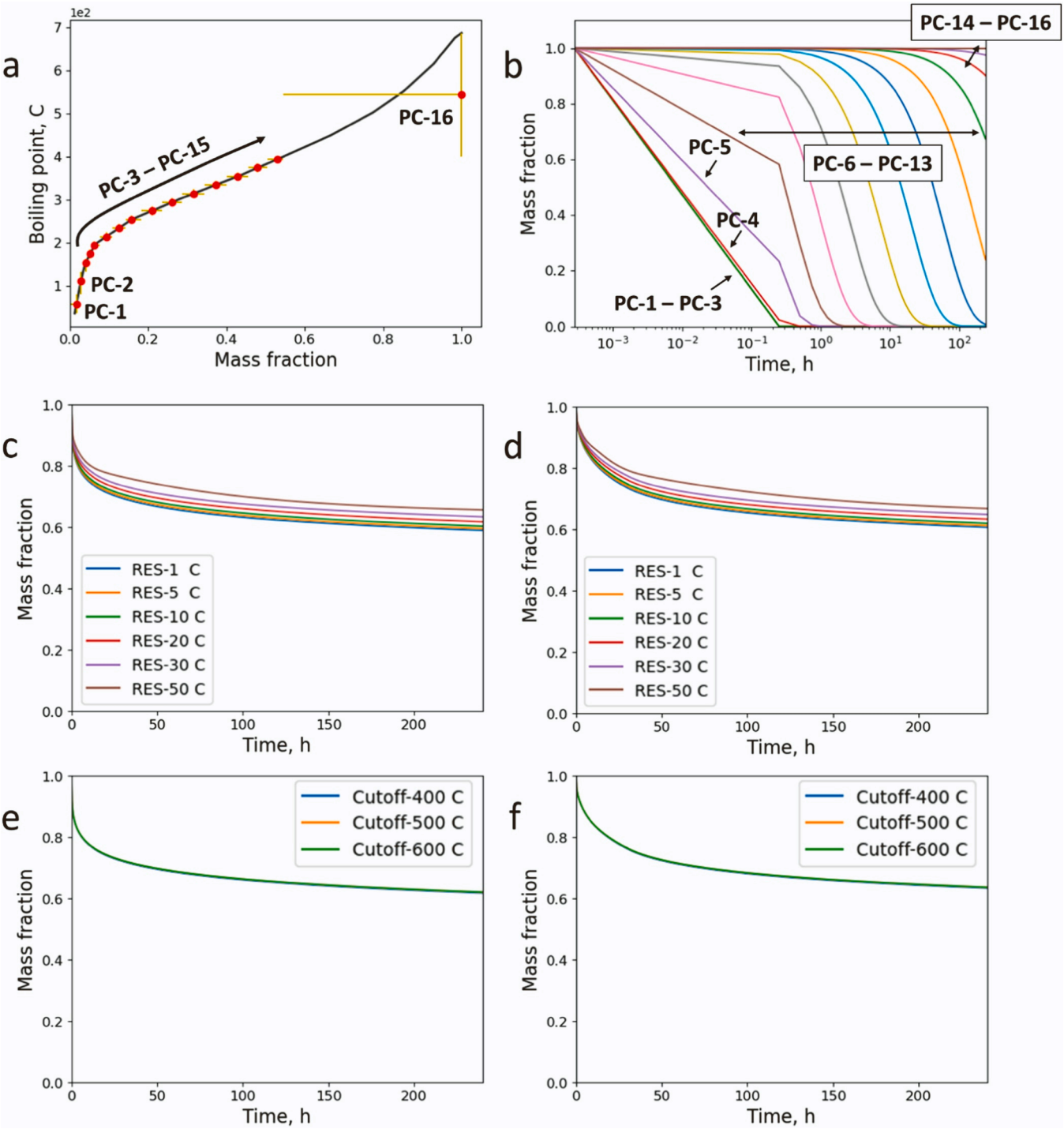

Fig. 7. : (a) Pseudo components constructed for the Heidrun crude oil with (temperature resolution, cutoff for high BPs) = (20 °C, 400 °C), and (b) simulated evaporation extent, taking into account oil spreading. (c-d) Simulated evaporation extent of the Heidrun crude oil using PCs constructed with different temperature resolutions for non-spreading and spreading cases, respectively. (e-f) Simulated evaporation extent of the Heidrun crude oil using PCs constructed with different cutoffs for high BPs for non-spreading and spreading cases, respectively.

perspective. It includes two PCs with low BPs, thirteen PCs with middle-range BPs constructed with a temperature resolution of 20 °C, and one PC with BP above 400 °C. Our findings of temperature thresholds for low and high BPs (i.e., 144 °C and 400 °C) are similar to those reported in [11]] which are 150 °C and 380 °C, respectively. For the PCs within the middle range of boiling temperature, out results suggest a finer resolution of 13 PCs in comparison to 7 PCs adopted in [11]. In this paper, it is important to acknowledge that we only utilized the constructed PCs to simulate the oil evaporative weathering process. However, it is crucial to recognize that various other physical and biochemical processes could occur during the transport of oil in the sea. These processes include natural dispersion, dissolution, and biodegradation, which are imperative to consider, especially for predicting the long-term oil weathering process. The approach for selecting PCs developed in this paper is founded on boiling temperature cuts, which holds potential for extending its application to model other oil weathering processes. For instance, [10] demonstrated that the solubility of light-weight aromatic components is strongly correlated with volatility

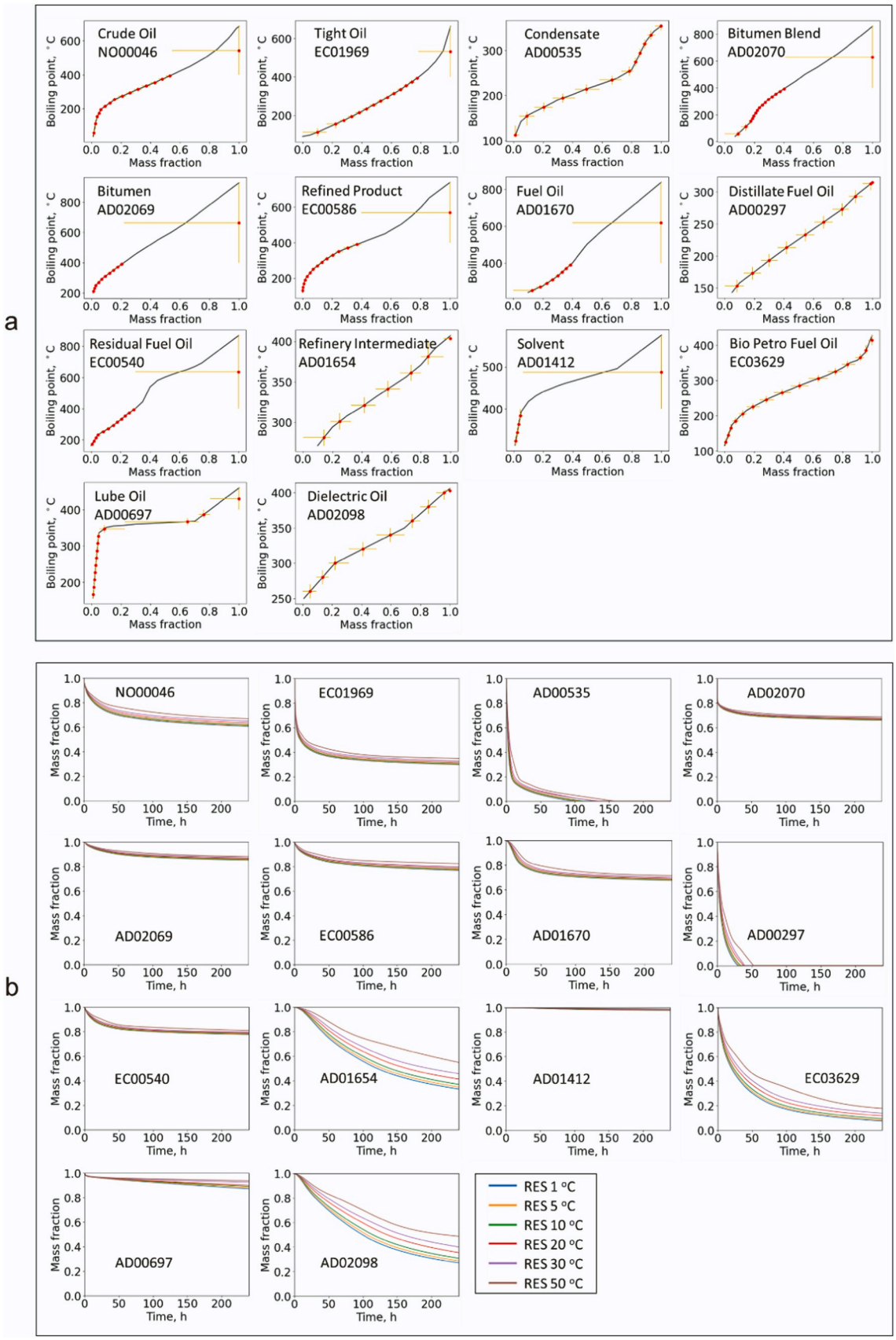

Fig. 8. (a) Examples of PCs constructed in 14 oil categories with (temperature resolution, cutoff for high BP) = (20 °C, 400 °C). (b) Comparison of the evaporation extent simulated by PCs constructed with different temperature resolutions.

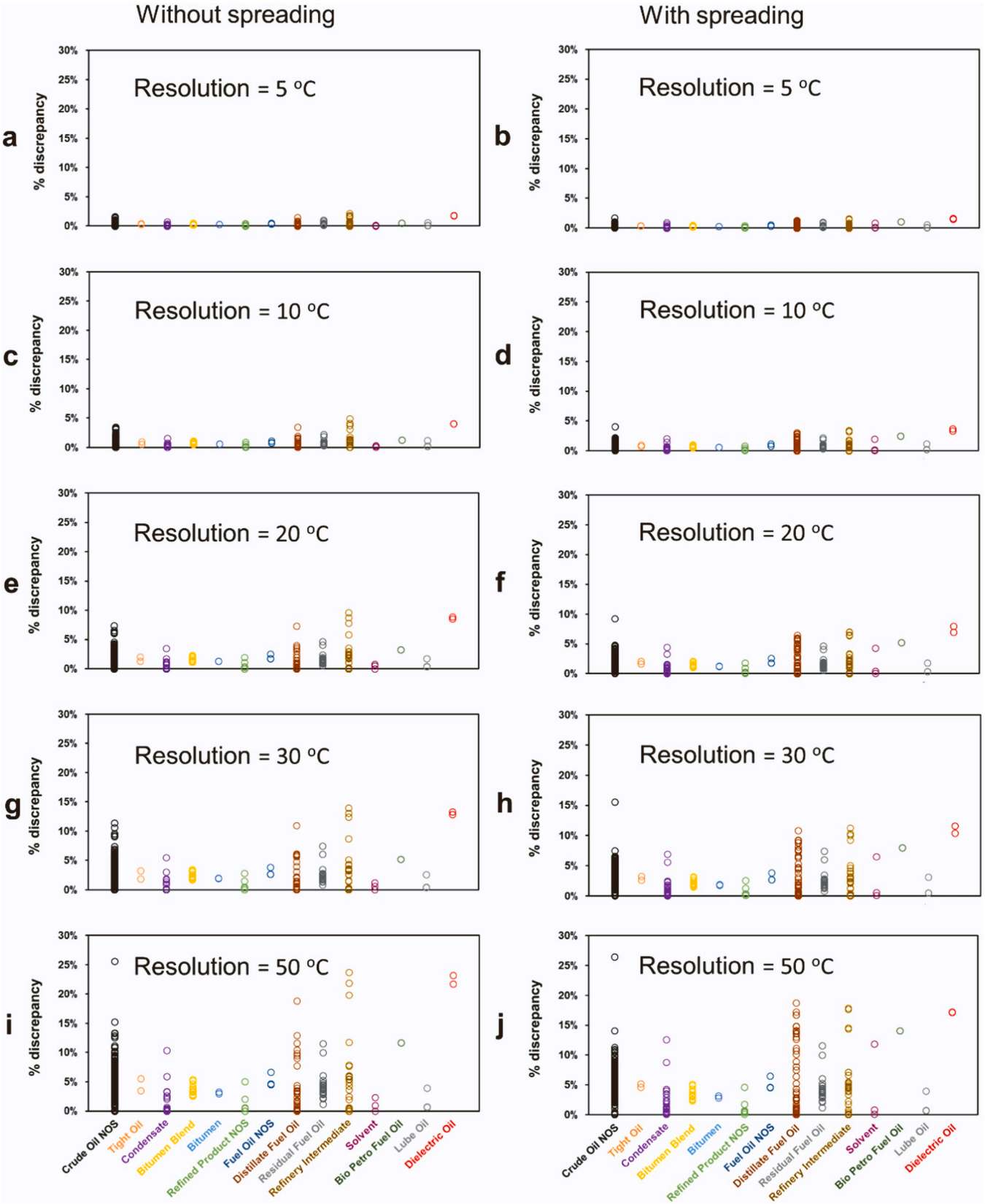

Fig. 9. : Percentage discrepancy of the simulated evaporation extent when the temperature resolution for constructing PCs of each oil becomes coarser from 1 °C to (a-b) 5 °C, (c-d) 10 °C, (e-f) 20 °C, (g-h) 30 °C, and (i and j) 50 °C without and with spreading, respectively. Note that the simulations were conducted for 899 oils characterized by 14 categories from the ADIOS database, and the % discrepancy is quantified as the ratio of the total oil mass loss over a 10 days' oil evaporation.

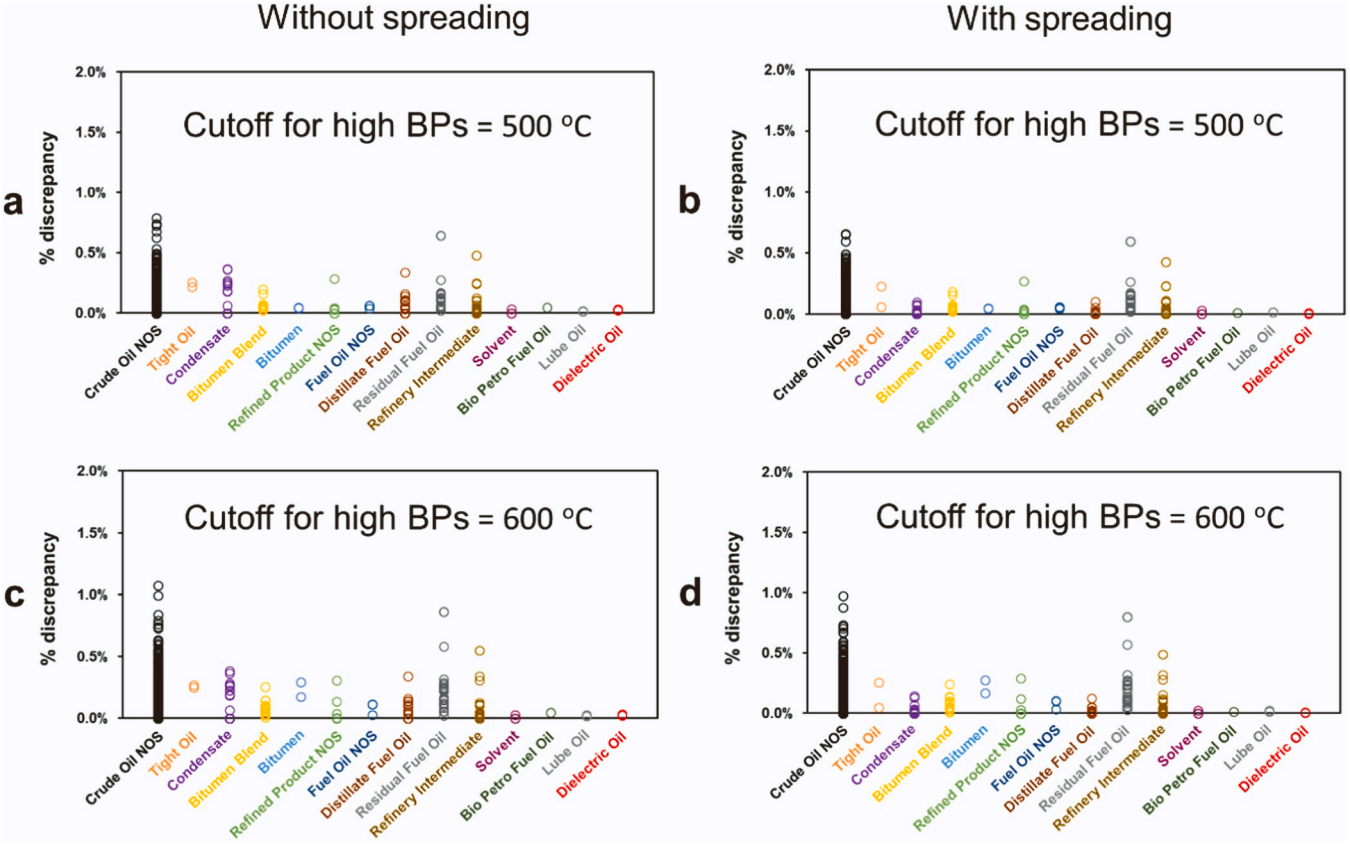

Fig. 10. : Percentage discrepancy of the simulated evaporation extent when the cutoff of high BPs increases from 400 °C to (a-b) 500 °C and (c-d) 600 °C without and with spreading, respectively. Note that the simulations were conducted for 899 oils characterized by 14 categories from the ADIOS database, and the % discrepancy is quantified as the ratio of the total oil mass loss over a 10 days' oil evaporation.

and thus can also be categorized using appropriate boiling cuts. Conversely, the dissolution of non-aromatic hydrocarbons is minimal and insignificant. In comparison to evaporation and dissolution, biodegradation occurs on a significantly longer time scale, which is typically considered for weathered oils. Geng et al., [14,15,16] approached the modeling of oil biodegradation by dividing oil into two major groups: long chain alkanes and polycyclic aromatic hydrocarbons (PAHs). The rationale behind this approach lies in the fact that low molecular weight (i.e., small chain) alkanes tend to evaporate rapidly [1], while low molecular weight aromatics, such as the single ring aromatics: benzene, toluene, ethylbenzene, and xylene (BTEX), exhibit relatively high solubility in water [34]. These two major groups are characterized by relatively high boiling points. Consequently, future research efforts can focus on constructing high-boiling-point PCs based on representative biodegradation rates of oil compound groups. This would enable the development of a consistent set of PCs capable of effectively simulating multiple oil weathering processes simultaneously. The PC approach presented in this paper sheds light on the development of effective modeling tools for forecasting oil weathering processes after oil spills.

4. Conclusion

In this paper, we developed a novel approach to construct the pseudo-components of oils which can be used to capture the complexity of the oil evaporative weathering process. The construction is classified into three categories: components with low BPs, mid-range BPs, and high BPs, respectively. The first PC includes the fraction from the initial BP to 80 °C to represent the compounds with BPs lower than benzene. The second PC includes the fraction from 80 °C to 144 °C to represent BTEX and whatever saturates fall in that range. One PC includes the fraction of high BP compounds, and its representative BP is the average of the threshold of high boiling temperature (e.g., 400 °C) and the terminal boiling temperature. The PCs with middle-range BPs are determined by a temperature resolution. Empirical formulas were derived to estimate the density and viscosity of PCs by fitting the curves to the ExxonMobil oil assays. The PC approach developed in this paper was tested and validated through the oil evaporation simulations conducted with multiple sets of PCs for 899 oils recorded in the ADIOS oil database. Our results suggest that the optimal number of PCs to adequately characterize oil evaporative weathering could be 16, determined by a temperature resolution of 20 °C and a cutoff of 400 °C for high BPs, with less than 10% discrepancy compared to that produced from 256 PCs constructed with 1-°C temperature resolution. This algorithm was written as part of the development of the new version of NOAA Emergency Response Division's GNOME oil spill modeling software, which could be useful for predicting evaporative weathering process for various types of oils.

Environmental Implication

Marine environments are at high risk from oil spills, and effective response and contingency planning for such spills relies on modeling of oil weathering. While pseudo component (PC) approach has been used for oil weathering modeling, a generic approach of constructing PCs to capture weathering processes for a wide range of oils has not yet been developed. To address this research gap, we developed an approach for constructing PCs based on oil distillation data. We validated the developed approach using 899 oils from the ADIOS oil library, and found an optimal number of PCs for capturing oil evaporative weathering.

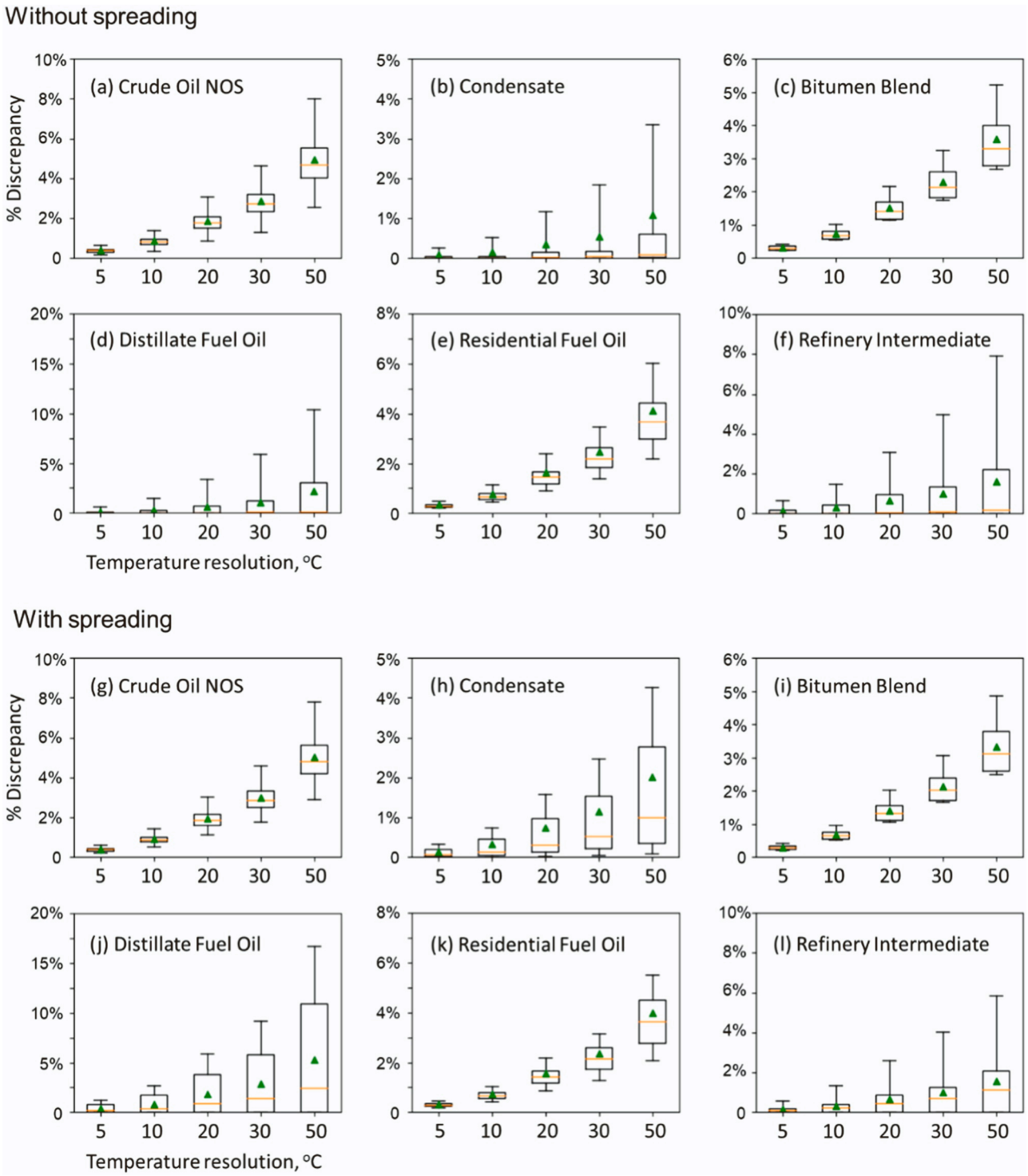

Fig. 11. : Boxplot of % the discrepancy of the simulated evaporation extent (a-f) without and (g-l) with spreading for the oil categories with over 10 oil records.

CRediT authorship contribution statement

Xiaolong Geng: Methodology, Formal analysis, Writing – original draft, Funding acquisition **Christopher H Barker**: Conceptualisation, Methodology, Supervision **Amy MacFadyen**: Supervision, Resources, Funding acquisition **Michel C. Boufadel**: Writing – review & editing, Funding acquisition. **Dalina L. Thrift-Viveros**: Conceptualisation, Methodology **Robert K Jones**: Conceptualisation, Methodology **Caitlin O'Connor**: Conceptualisation, Methodology **Kenneth Lee**: Resources, Funding acquisition.

Declaration of Competing Interest

The authors declare that they have no known competing financial interests or personal relationships that could have appeared to influence the work reported in this paper.

Acknowledgment

This work was funded by the United States National Science Foundation (Division of Earth Sciences [EAR] Grant ID: #2130595. However,

it does not necessarily reflect the views of the funding agency, and no official endorsement should be inferred. This is SOEST contribution #11708.

Appendix A. Supporting information

Supplementary data associated with this article can be found in the online version at doi:10.1016/j.jhazmat.2023.132160.

References

[1] Atlas, R.M., Hazen, T.C., 2011. Oil biodegradation and bioremediation: a tale of the two worst spills in U.S. History. Environ Sci Technol 45 (16), 6709–6715.
[2] Baker, M.C., Steinhoff, M.A., Fricano, G.F., 2017. Integrated effects of the deepwater horizon oil spill on nearshore ecosystems. Mar Ecol Prog Ser 576, 219–234.
[3] Barker, C.H., Kourafalou, V.H., Beegle-Krause, C., Boufadel, M., Bourassa, M.A., Buschang, S.G., et al., 2020. Progress in operational modeling in support of oil spill response. J Mar Sci Eng 8 (9), 668.
[4] Blokker, P., 1964. Spreading and evaporation of petroleum products on water, In: Proceedings of the 4th International Harbour Conference, Antwerp, Belgium (1964), edited, pp. 911–919.
[5] Bodkin, J.L., Ballachey, B.E., Coletti, H.A., Esslinger, G.G., Kloecker, K.A., Rice, S. D., et al., 2012. Long-term effects of the 'Exxon Valdez'oil spill: sea otter foraging in the intertidal as a pathway of exposure to lingering oil. Mar Ecol Prog Ser 447, 273–287.
[6] Boufadel, M.C., Abdollahi-Nasab, A., Geng, X., Galt, J., Torlapati, J., 2014. Simulation of the landfall of the deepwater horizon oil on the shorelines of the Gulf of Mexico. Environ Sci Technol 48 (16), 9496–9505.
[7] Buchanan, I., Hurford, N., 1988. Methods for predicting the physical changes in oil spilt at sea. Oil Chem Pollut 4 (4), 311–328.
[8] Butler, J., 1976. Transfer of petroleum residues from sea to air: evaporative weathering. In: Windom, H.L., Duce, R.A. (Eds.), Marine Pollutant Transfer. Lexington Books, Toronto, pp. 201–212 (edited).
[9] Fingas, M., 2015. Oil and petroleum evaporation. Handb Oil Spill Sci Technol 2 (3), 205–223.
[10] French-McCay, 2003. Development and application of damage assessment modeling: example assessment for the North Cape oil spill. Mar Pollut Bull 47 (9–12), 341–359.
[11] French-McCay, D.P., Jayko, K., Li, Z., Spaulding, M.L., Crowley, D., Mendelsohn, D., et al., 2021. Oil fate and mass balance for the Deepwater Horizon oil spill. Mar Pollut Bull 171, 112681.
[12] French-McCay, D.P., Spaulding, M.L., Crowley, D., Mendelsohn, D., Fontenault, J., Horn, M., 2021. Validation of oil trajectory and fate modeling of the deepwater horizon oil spill. Front Mar Sci 8, 618463.
[13] French McCay, D., K. Jayko, Z. Li, M. Horn, Y. Kim, T. Isaji, D. Crowley, M. Spaulding, L. Decker, and C. Turner, 2015. Technical Reports for Deepwater Horizon Water Column Injury Assessment–WC_TR14: Modeling Oil Fate and Exposure Concentrations in the Deepwater Plume and Cone of Rising Oil Resulting from the Deepwater Horizon Oil Spill, DWH NRDA Water Column Technical Working Group Report. Prepared for National Oceanic and Atmospheric Administration by RPS ASA, South Kingstown, RI, USA, 29.
[14] Geng, X., Boufadel, M.C., Personna, Y.R., Lee, K., Tsao, D., Demicco, E.D., 2014. BioB: a mathematical model for the biodegradation of low solubility hydrocarbons. Mar Pollut Bull 83 (1), 138–147.
[15] Geng, X., Boufadel, M.C., Lee, K., Abrams, S., Suidan, M., 2015. Biodegradation of subsurface oil in a tidally influenced sand beach: impact of hydraulics and interaction with pore water chemistry. Water Resour Res 51 (5), 3193–3218.
[16] Geng, X., Pan, Z., Boufadel, M.C., Ozgokmen, T., Lee, K., Zhao, L., 2016. Simulation of oil bioremediation in a tidally influenced beach: spatiotemporal evolution of nutrient and dissolved oxygen. J Geophys Res: Oceans 121 (4), 2385–2404.
[17] Geng, X., C. Abou Khalil, R.C. Prince, K. Lee, C. An, and M.C. Boufadel , 2021, Hypersaline pore water in Gulf of Mexico beaches prevented efficient biodegradation of Deepwater Horizon beached oil, Environmental science & technology accepted.
[18] Geng, X., Boufadel, M.C., Rajaram, H., Cui, F., Lee, K., An, C., 2020. Numerical study of solute transport in heterogeneous beach aquifers subjected to tides. Water Resour Res 56 (3) e2019WR026430.
[19] Hamoda, M., Hamam, S., Shaban, H., 1989. Volatilization of crude oil from saline water. Oil Chem Pollut 5 (5), 321–331.
[20] Jones, R. , 1997. A simplified pseudo-component oil evaporation model. Paper presented at Proceedings of the 20th Arctic and Marine Oil Spill Program (AMOP) Technical Seminar, Environment Canada.
[21] Lehr, W., Jones, R., Evans, M., Simecek-Beatty, D., Overstreet, R., 2002. Revisions of the ADIOS oil spill model. Environ Model Softw 17 (2), 189–197.
[22] Lehr, W.J., 2001. Review of modeling procedures for oil spill weathering behavior. Adv Ecol Sci 9, 51–90.
[23] Lehr, W.J., 2021. A brief survey of oil spill weathering models. Mar Hydrocarb Spill Assess 27–57.
[24] Li, P., Niu, H., Li, S., King, T.L., Zou, S., Chen, X., et al., 2022. DBWM: A diluted bitumen weathering model. Mar Pollut Bull 175, 113372.
[25] Lyman, W.J. , W.F. Reehl , and D.H. Rosenblatt , 1990. Handbook of chemical property estimation methods.
[26] MacFadyen, A. , 2017. Modeling transport of oil from the Refugio Beach oil spill, Paper presented at International Oil Spill Conference Proceedings, International Oil Spill Conference.
[27] Mackay, D., Matsugu, R.S., 1973. Evaporation rates of liquid hydrocarbon spills on land and water. Can J Chem Eng 51 (4), 434–439.
[28] Mishra, A.K., Kumar, G.S., 2015. Weathering of oil spill: modeling and analysis. Aquat Procedia 4, 435–442.
[29] Payne, J., B. Kirstein, G. McNabb Jr, J. Lambach, R. Redding, R. Jordan, W. Hom, C. De Oliveira, G. Smith, and D. Baxter, 1984. Multivariate analysis of petroleum weathering in the marine environment–sub Arctic, Environmental Assessment of the Alaskan Continental Shelf, Final Report of Principal Investigators, 21, 423–434.
[30] Payne, J. , G. McNabb , L. Hachmeister , B. Kirstein , and J. Clayton , 1987. Development of a predictive model for the weathering of oil in the presence of sea ice.
[31] Payne, J.R., 1984. Weathering of petroleum in the marine environment. Mar Technol Soc J 18, 24–42.
[32] Payne, J.R. , B.E. Kirstein , G.D. McNabb Jr , J.L. Lambach , C. de Oliveira , R.E. Jordan , et al. , 1983. Multivariate analysis of petroleum hydrocarbon weathering in the subarctic marine environment, paper presented at International Oil Spill Conference, American Petroleum Institute.
[33] Quinn, M., Marron, K., Patel, B., Abu-Tabanja, R., Al-Bahrani, H., 1990. Modelling of the ageing of crude oils. Oil Chem Pollut 7 (2), 119–128.
[34] Reddy, C.M., et al., 2012. Composition and fate of gas and oil released to the water column during the Deepwater Horizon oil spill. Proc Natl Acad Sci USA 109 (50), 20,229–20,234.
[35] Reuscher, M.G., Baguley, J.G., Conrad-Forrest, N., Cooksey, C., Hyland, J.L., Lewis, C., et al., 2017. Temporal patterns of Deepwater Horizon impacts on the benthic infauna of the northern Gulf of Mexico continental slope. PLOS One 12 (6), e0179923.
[36] Riazi, M., 2005. Characterization and Properties of Petroleum Fractions. ASTM International,, Philadelphia.
[37] Tkalin, A., 1986. Evaporation of petroleum hydrocarbons from films on a smooth sea surface. Oceanology 26 (4), 473–474.
[38] Ülker, D., Burak, S., Balas, L., Çağlar, N., 2022. Mathematical modelling of oil spill weathering processes for contingency planning in Izmit Bay. Reg Stud Mar Sci 50, 102155.
[39] Vaz, A.C., Paris, C.B., Dissanayake, A.L., Socolofsky, S.A., Gros, J., Boufadel, M.C., 2020. Dynamic coupling of near-field and far-field models. Deep Oil Spills. Springer,, pp. 139–154.
[40] Wolfe, D., Michel, J., Hameedi, M., Payne, J., Galt, J., Watabayashi, G., et al., 1994. The fate of the oil spilled from the Exxon Valdez. Environ Sci Technol 28 (13), 560A–568A.
[41] Zelenke, B. , C. O'Connor , C.H. Barker , C. Beegle-Krause , and L. Eclipse , 2012. General NOAA operational modeling environment (GNOME) technical documentation, U.S. Dept. of Commerce, NOAA Technical Memorandum NOS OR and R 40., Seattle, WA: Emergency Response Division, NOAA.
[42] Zhong, X., Niu, H., Li, P., Wu, Y., Liu, L., 2022. An overview of oil-mineral-aggregate formation, settling, and transport processes in marine oil spill models. J Mar Sci Eng 10 (5), 610.
[43] Zodiatis, G., Lardner, R., Spanoudaki, K., Sofianos, S., Radhakrishnan, H., Coppini, G., et al., 2021. Operational oil spill modelling assessments. Marine Hydrocarbon Spill Assessments. Elsevier,, pp. 145–197.